INTRODUCTION

The sound produced by the trombone may be seen as the coupling of the input pressure from the lips (the product of the volume velocity output from a pressure-controlled valve and the bore's characteristic impedance) with the instrument mouthpiece, bore and bell. In this work, the current status of trombone physical modelling, and the synthesis and/or measurement of these components, is presented.

TROMBONE BORE AND BELL

Though wave propagation in many wind instruments bores may be modeled as a one-dimensional waveguide, more attention is required when the bore departs from a purely cylindrical or conical contour—such as at the mouthpiece (discussed in Section 4) and at the bell (discussed herein).

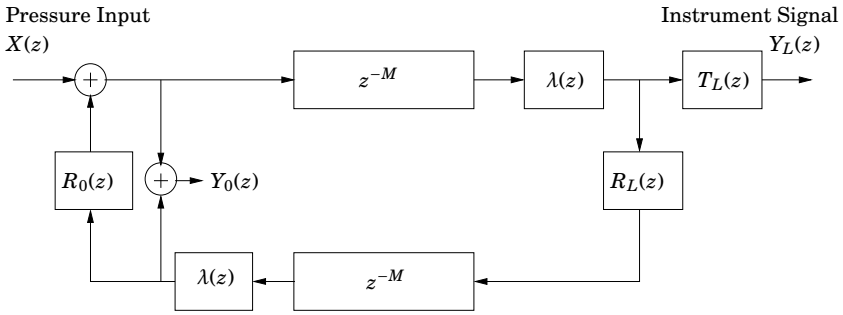

FIGURE 1: Waveguide model of a cylindrical tube with commuted propagation loss filters $\lambda(z)$, open-end terminating reflection and transmission filters $R_L(z)$ and $T_L(z)$ respectively, and a reflection filter $R_0(z)$ at the (effectively) closed end termination corresponding to the position of the mouthpiece (a more accurate accounting of the mouthpiece is developed in Section 4). The model is tapped at two observation points: the bore base, producing $Y_0(z)$, and the instrument output, producing $Y_L(z)$, in response to input pressure $X(z)$.

The model depicted in Figure 1 has several filter elements describing the acoustic characteristics of the system that may, or may not, change over time:

- **The delay of M samples** accounts for the acoustic propagation delay in the bore, the value typically being set according to the bore's effected length or the desired sounding pitch.
- **Propagation/wall losses** $\lambda(z)$ are well described theoretically [1, pp. 193-196], with a parametric filter described in [2], allowing for real-time changes according to tube size and length.
- **The reflection and transmission at the bell, $R_L(z)$ and $T_L(z)$**, respectively, may be derived either from a computational model or from measurement (see Figure 2), with the former emphasizing parametrization and ability to change the bell contour during performance, and with the latter offering assumed greater accuracy. Because the trombone bell is not expected to change during performance, and because it disassembles easily from the trombone bore, its reflection and transmission functions may be estimated using the measurement technique described in [3].
- **The reflection at the mouthpiece position $R_0(z)$.** As this is expected to change during performance with the vibrating lips changing both the mouthpiece volume and the opening to the bore, this waveguide element is not easily measured but better developed within the context of coupling with the dynamic lip reed model and mouthpiece, discussed in Section 3 and 4.

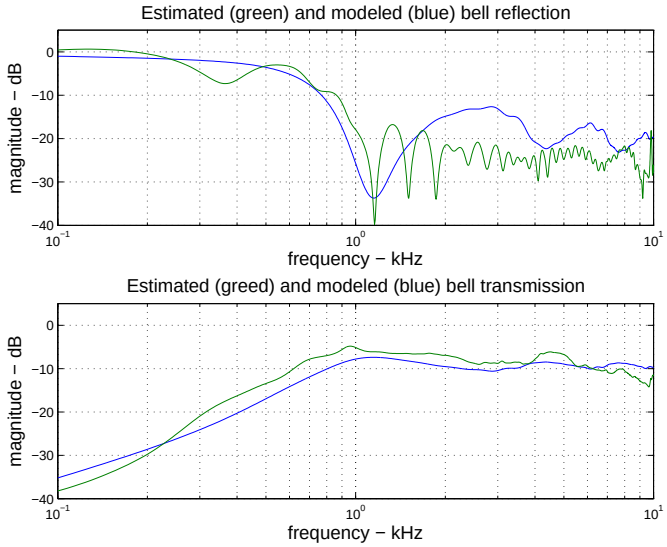

FIGURE 2: Estimated and modeled bell reflection and transmission magnitudes as in [3].

LIP VALVE MODEL

When blowing into a trombone, air pressure from the lungs/mouth creates a pressure difference across the surface of the lips, causing them to vibrate. The oscillation of vibrating lips in a brass instrument is typically characterized as being "blown open" [4], and strongly coupled to the bore, making playability (*regular* non-chaotic oscillation of lips), highly dependent on the resonances of the bore and bell.

Here, the generalized pressure-controlled valve model, first introduced in [5], is used in its "blown-open" configuration as illustrated in Figure 3. The displacement of the valve is given by its angle θ from the vertical axis and the valve classification is determined by 1) its initial position θ_0 (its equilibrium position in the absence of flow), and 2) by the use of an optional *stop*—a numerical limit placed to constrain the range of θ. Since the stop is placed at the center vertical axis, $\theta = 0$, and the initial equilibrium position of the valve θ_0 is to the right of the stop, $\theta_0 > 0$, an increased blowing pressure will cause the reed to *blow open*.

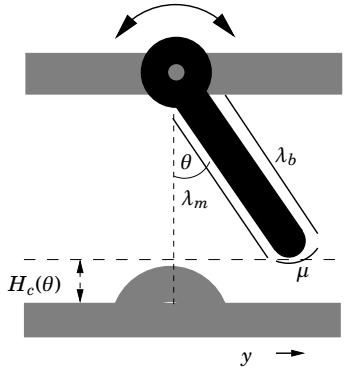

FIGURE 3: The blown open configuration of the generalized valve model, showing geometric parameters λ_m, the length of the valve that sees the mouth pressure, λ_d, the length of the valve that sees the valve's downstream pressure, and μ, the length of the valve that sees the flow. Changing these parameters will change the corresponding component forces of the overall driving force $F = F_m + F_b + F_U$.

As the reed angle θ changes during oscillation, the valve opening area A changes according to

$$A(\theta) = wH_c(\theta), \tag{1}$$

where w is the width of the channel and $H_c(\theta)$ is the channel height, which may be specified by a number of possible functions, such as

$$H_c(\theta) = 1 - \cos\theta, \tag{2}$$

suitable for lip reeds.

The geometry of the valve may be further specified by setting the effective length of the reed that sees the mouth pressure λ_m, the reed length that sees the bore pressure λ_b, and the reed length that sees the flow, given by μ (see Figure 3). These variables have an audible effect on the overall driving force acting on the reed, given by F in (3), and can be seen as offering finer control of embouchure.

Once the valve is set into motion, the value for θ is determined by the second order differential equation

$$m\frac{d^2\theta(t)}{dt^2} + m2\gamma\frac{d\theta(t)}{dt} + k(\theta(t) - \theta_0) = F, \tag{3}$$

where m is the effective mass of the reed, γ is the damping coefficient, k is the stiffness of the reed, and F is the overall driving force acting on the reed, a function of the mouth and bore pressure, and flow in contact with the reed. The frequency of vibration for this mode is given by $\omega_v = \sqrt{k/m - \gamma^2}$.

Discretization, equivalent to applying a bilinear transform, yields the transfer function in the z domain

$$\frac{\theta(z)}{F(z) + k\theta_0} = \frac{1 + 2z^{-1} + z^{-2}}{a_0 + a_1 z^{-1} + a_2 z^{-2}}, \tag{4}$$

and the corresponding difference equation

$$\theta(n) = [F_k(n) + 2F_k(n-1) + F_k(n-2) - a_1\theta(n-1) - a_2\theta(n-2)]/a_0, \tag{5}$$

where $F_k(n) = F(n) + k\theta_0$, and

$$\begin{aligned} a_0 &= m\alpha^2 + mg\alpha + k, \\ a_1 &= -2(m\alpha^2 - k), \\ a_2 &= m\alpha^2 - mg\alpha + k, \end{aligned}$$

and $\alpha = 2/T$, where T is the sampling period, and $g = 2\lambda$. Since pole frequencies are well below half the sampling rate, there is no need for pre-warping.

The force driving the reed F is equal to the sum of the forces acting on the reed, $F = F_m + F_b + F_U$, where $F_m = w\lambda_m p_m$ is the force acting (in the positive θ direction) on the surface area $\lambda_m w$, $F_b = -w\lambda_b p_b$, is the force acting (in the negative θ direction) on the surface area $\lambda_b w$, and F_U is the force applied by the flow (which forces the reed open) given by

$$F_U = \text{sign}(\theta) w\mu\left(p_m - \frac{\rho}{2}\left(\frac{U(t)}{A(t)}\right)^2\right). \tag{6}$$

As can be seen by (6), the total force driving the reed is dependent on the valve classification, since the sign of θ is determined by its limits.

The differential equation governing air flow through the valve, fully derived in [6], is given by

$$\frac{dU(t)}{dt} = (p_m - p_b)\frac{A(t)}{\mu\rho} - \frac{U(t)^2}{2\mu A(t) + U(t)T}. \tag{7}$$

where p_m is mouth pressure, p_b is the bore pressure (see discussion in the following section), $A(t)$ is the cross sectional area of the valve channel, and μ is the length of reed that sees the

flow. Equation (7) is used to update the flow U every sample period (given by the inverse of the sampling rate).

There are, therefore, three variables that evolve over time in response to an applied mouth pressure p_m: the displacement of the reed θ (determined using 5), the flow U, determined using the update given by (7), and the pressure at the base of the bore p_b, obtained from the waveguide model as shown in Figure 1.

TABLE 1: Example parameters values for the lip reed.

Quantity	Variable	Value
Radius of exhaust	a	8 mm
Valve width	w	2.3 mm
Valve length	$\lambda_m = \lambda_b$	23.2 mm
Valve mass	m	.3 g
Valve thickness	ν	6 mm
Initial displacement	θ_0	0.01 mm
Mouthpiece volume	V	5×10^{-6} m^3
Mouthpiece choke length	l_c	48 cm
Mouthpiece choke radius	a_c	4.5 mm

MOUTHPIECE

Connecting the lip model to the instrument is done via the mouthpiece to account for the resonance created by the mouthpiece's cup volume and its backbore constriction.

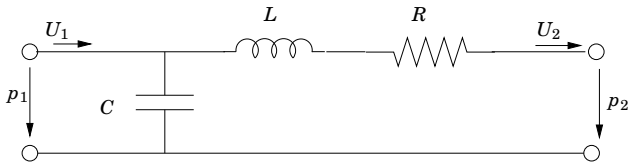

FIGURE 4: The system diagram for the mouthpiece model. The cup volume is represented by the capacitor, and the attached narrow constriction is modeled as a series inertance L and dissipative element R, which accounting for wall losses.

As shown in [1, 7] and others, the mouthpiece may be modeled by the equivalent electrical circuit shown in Figure 4. The mouthpiece consists of a cup having a volume V, and presents an acoustic compliance C given by

$$C = \frac{V}{\rho c^2}, \tag{8}$$

where ρ is the air density and c is the velocity of sound in air. The cup is followed by a constricted passage before entering into the wider trombone bore, with the constriction behaving as a series inertance (inductance in electrical terms) given by

$$L = \frac{\rho l_c}{S_c}, \tag{9}$$

where l_c is the length and S_c is the cross-sectional area of the constriction. The dissipative element R in series with this inertance represents viscous and thermal losses. Its value for the mouthpiece has been obtained through experiment in [8].

Inserting a mouthpiece between the reed and bore models requires a new expression for the volume flow entering the bore (it is no longer that coming directly from the lips), as well as a new

expression for the downstream pressure used when in the dynamic lip reed model (it is no longer the bore base pressure). These quantities are termed $U_2(t)$ and $p_1(t)$, respectively, in Figure 4.

The mouthpiece model provides a volume flow $U_2(t)$ into the bore and a pressure $p_1(t)$ in the mouthpiece, in response to a volume flow $U_1(t)$ entering the mouthpiece (generated by the lip reed model) affixed to the instrument having a pressure of $p_2(t)$ at the bore base.

Taking the Laplace transform of the differential equations describing the mouthpiece model in Figure 4 leads to the system's frequency domain input-output matrix

$$\begin{bmatrix} U_1(s) \\ p_1(s) \end{bmatrix} = \begin{bmatrix} s^2LC + sRC + 1 & sC \\ sL + R & 1 \end{bmatrix} \begin{bmatrix} U_2(s) \\ p_2(s) \end{bmatrix}, \tag{10}$$

which may be rearranged and discretized to yield expressions for U_2 and p_1 in response to U_1 and p_2, given in the z-domain as

$$U_2(z) = \frac{U_1(z)(1 + 2z^{-1} + z^{-2}) - C\alpha p_2(z)(1 - z^{-2})}{a_{m0} + a_{m1}z^{-1} + a_{m2}z^{-2}}, \tag{11}$$

where

$$\begin{aligned} a_{m0} &= LC\alpha^2 + RC\alpha + 1 \\ a_{m1} &= -2(LC\alpha^2 - 1) \\ a_{m2} &= LC\alpha^2 - RC\alpha + 1 \end{aligned}$$

and

$$p_1(z) = \frac{U_2(z)(b_0 + b_1z^{-1}) + p_2(z)(1 + z^{-1})}{1 + z^{-1}}, \tag{12}$$

where

$$b_0 = L\alpha + R \quad \text{and} \quad b_1 = -L\alpha + R,$$

and $\alpha = 2/T$, where T is the sampling period. The corresponding difference equations are given by

$$\begin{aligned} U_2(n) = {} & [U_1(n) + 2U_1(n-1) + U_1(n-2) - \\ & C\alpha(p_2(n) - p_2(n-2)) - \\ & a_1U_2(n-1) - a_2U_2(n-2)]/a_0, \end{aligned}$$

and

$$\begin{aligned} p_1(n) = {} & b_0U_2(n) + b_1U_2(n-1) + \\ & p_2(n) + p_2(n-1) - p_1(n-1). \end{aligned}$$

Again, as for the case of discretizing the valve displacement, no pre-warping is required. The effects of the mouthpiece can be viewed by comparing the model's output with and without a mouthpiece, with all other parameters set as in Table 1.

CONCLUSIONS

This work assembles recent contributions to trombone synthesis. A measurement technique, shown to produce accurate data for wind instrument bells, is combined with waveguide synthesis, a generalized pressure-controlled valve model configured to act as a lip reed, and an existing mouthpiece model to produce a quality real-time parametric trombone model.

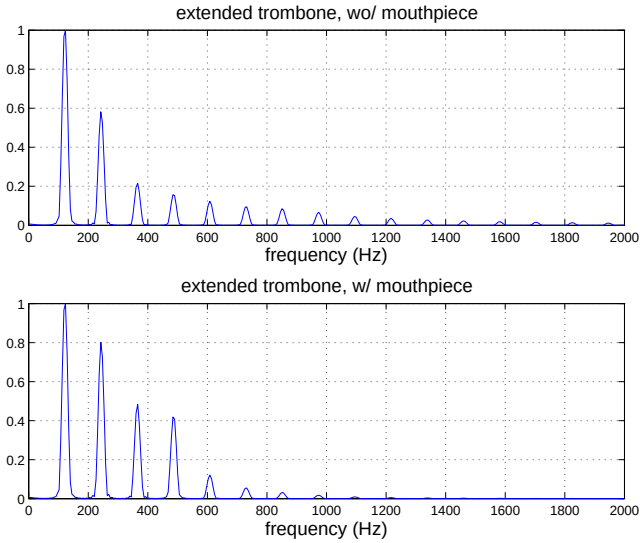

FIGURE 5: The magnitude spectrum of the model output showing the resonant effects of the mouthpiece.

ACKNOWLEDGMENTS

The authors are sincerely grateful to the Natural Sciences and Engineering Research Council of Canada (NSERC) for their support through the Discovery program.

REFERENCES

[1] N. H. Fletcher and T. D. Rossing, *The Physics of Musical Instruments* (Springer-Verlag) (1995).

[2] J. Abel, T. Smyth, and J. O. Smith, "A simple, accurate wall loss filter for acoustic tubes", in *DAFX 2003 Proceedings*, 53–57 (International Conference on Digital Audio Effects, London, UK) (2003).

[3] T. Smyth and F. S. Scott, "Trombone synthesis by model and measurement", EURASIP Journal on Advances in Signal Processing **2011**, 13 pages (2011), doi:10.1155/2011/151436.

[4] N. H. Fletcher, "Autonomous vibration of simple pressure-controlled valves in gas flows", Jounal of the Acoustical Society of America **93**, 2172–2180 (1993).

[5] T. Smyth, J. Abel, and J. O. Smith, "A generalized parametric reed model for virtual musical instruments", in *Proceedings of ICMC 2005*, 347–350 (International Computer Music Conference, Barcelona, Spain) (2005).

[6] T. Smyth, J. Abel, and J. O. Smith, "The feathered clarinet reed", in *Proceedings of the International Conference on Digital Audio Effects (DAFx'04)*, 95–100 (Naples, Italy) (2004).

[7] M. van Walstijn, "Discrete-time modelling of brass and reed woodwind instruments with application to musical sound synthesis", Ph.D. thesis, University of Edinburgh (2002).

[8] P. Dietz, "Simulation of trumpet tones via physical modeling", Master's thesis, Dept. of Electrical Engineering, Bucknell University, Lewisburg, USA (1988).